



Long-term strain improvements accumulate mutations in regulatory elements responsible for hyper-production of cellulolytic enzymes

SUBJECT AREAS:

INDUSTRIAL
MICROBIOLOGY

GENE EXPRESSION PROFILING

FUNGAL SYSTEMS BIOLOGY

REVERSE ENGINEERING

Received
5 February 2013

Accepted
13 March 2013

Published
28 March 2013

Guodong Liu^{1*}, Lei Zhang^{2*}, Yuqi Qin^{1,3*}, Gen Zou^{2*}, Zhonghai Li^{1*}, Xing Yan², Xiaomin Wei¹, Mei Chen¹, Ling Chen², Kai Zheng¹, Jun Zhang², Liang Ma², Jie Li¹, Rui Liu², Hai Xu¹, Xiaoming Bao¹, Xu Fang^{1,3}, Lushan Wang¹, Yaohua Zhong¹, Weifeng Liu¹, Huajun Zheng⁴, Shengyue Wang⁴, Chengshu Wang², Luying Xun^{1,5}, Guo-Ping Zhao^{2,4}, Tianhong Wang¹, Zhihua Zhou² & Yinbo Qu^{1,3}

¹State Key Laboratory of Microbial Technology, Shandong University, Jinan, Shandong, China, ²Key Laboratory of Synthetic Biology, Institute of Plant Physiology and Ecology, Shanghai Institutes for Biological Sciences, Chinese Academy of Sciences, Shanghai, China, ³National Glycoengineering Research Center, Shandong University, Jinan, Shandong, China, ⁴Shanghai-MOST Key Laboratory of Disease and Health Genomics, Chinese National Human Genome Center at Shanghai, Shanghai, China, ⁵School of Molecular Biosciences, Washington State University, Pullman, WA, USA.

Correspondence and requests for materials should be addressed to G.-P.Z. (gpzhao@sibs.ac.cn); T.H.W. (wangtianhong@sdu.edu.cn); Z.H.Z. (zhouzhihua@sippe.ac.cn) or Y.B.Q. (quyinbo@sdu.edu.cn)

* These authors contributed equally to this work.

Long-term strain improvements through repeated mutagenesis and screening have generated a hyper-producer of cellulases and hemicellulases from *Penicillium decumbens* 114 which was isolated 30 years ago. Here, the genome of the hyper-producer *P. decumbens* JU-A10-T was sequenced and compared with that of the wild-type strain 114-2. Further, the transcriptomes and secretomes were compared between the strains. Selective hyper-production of cellulases and hemicellulases but not all the secreted proteins was observed in the mutant, making it a more specific producer of lignocellulolytic enzymes. Functional analysis identified that changes in several transcriptional regulatory elements played crucial roles in the cellulase hyper-producing characteristics of the mutant. Additionally, the mutant showed enhanced supply of amino acids and decreased synthesis of secondary metabolites compared with the wild-type. The results clearly point out that we can target gene regulators and promoters with minimal alterations of the genetic content but maximal effects in genetic engineering.

The rapid increase in crude oil prices and decrease in crude oil reserves have significantly stimulated the search and use of renewable resources and energy. Lignocellulosic materials from agriculture and forest by-products are relatively abundant renewable resources. The use of lignocellulosic biomass for the production of liquid fuels and chemicals has long been considered to be an important alternative for sustaining the human economy and society^{1,2}. In one of the most common biorefinery schemes, lignocellulosic materials are partially treated by physical and chemical methods to release cellulose and hemicellulose which then are hydrolyzed to fermentable sugars by a lignocellulolytic enzyme system consisting of multiple cellulases and hemicellulases. The sugars can be converted to ethanol or other products^{2,3}.

Although recombinant protein expression technology has been applied to the production of most industrial enzymes, lignocellulolytic enzyme systems are primarily produced by fungi that are often enhanced through strain improvement^{4,5}. The most widely used commercial lignocellulolytic enzymes are produced by *Trichoderma reesei* strains that have been improved through repeated mutagenesis and screening⁶. Mutations in three genes, carbon repressor gene *cre1* (ref. 7), β -glucosidase regulator gene *bglR*⁸ and glucosidase II α subunit gene *gls2 α* ⁹, contribute to the hyper-production of cellulolytic enzymes in *T. reesei* mutant strains. Mutations in *cre1* and *bglR* lead to reduced carbon catabolite repression, and the mutated *gls2 α* results in altered N-glycan patterns on secreted proteins. Although high numbers of genetic mutations have been found in several *T. reesei* mutants through comparative genomics analysis^{10,11}, additional mechanisms accounting for the hyper-producing phenotype remain enigmatic.



Some *Penicillium* species have been reported to produce more balanced native lignocellulolytic enzyme systems than *T. reesei*¹², and our previous study indicated that there were more diverse genes encoding cellulose binding domain-containing proteins and hemicellulases in the genome of cellulolytic fungus *Penicillium decumbens* than those in *T. reesei*¹³. The original *P. decumbens* isolate 114 was obtained from decayed straw-covered soil in 1979 (ref. 14), and has been improved through a series of mutagenesis and screening over the years (Fig. 1A). Carbon catabolite repression (CCR)-resistant strain UV11 was first obtained by selecting a mutant forming a clear halo zone on a holocellulose-glucose agar plate¹⁴. Multiple rounds of further mutagenesis and selection generated JU-A10 (ref. 15), followed by JU-A10-T, which has been used for industrial-scale cellulase production in China for 17 years with a productivity of 160 IU L⁻¹ h⁻¹ (ref. 16). The activities of the lignocellulolytic enzyme system of JU-A10-T increased several times compared to those of the sequenced strain 114-2. However, the molecular mechanisms behind the strain improvement for higher cellulase production are poorly understood.

In this study, comparative and functional genomics studies of *P. decumbens* mutant JU-A10-T and wild-type strain 114-2 were performed to decipher how strain improvement has significantly improved the production of the lignocellulolytic enzyme system. Mutations in gene regulators and promoter regions partially accounted for the increased production of cellulases and hemicellulases. Transcriptome analysis further revealed clues for the hyper

production of lignocellulolytic enzymes in the mutant. Collectively, the results offer a multi-level understanding of enzyme hyper-production by *P. decumbens* strain JU-A10-T, and the findings will provide guidance for targeted genetic modification to enhance the production of lignocellulolytic enzymes.

Results

The different phenotypes between wild-type strain 114-2 and mutant JU-A10-T. The mutant JU-A10-T produces ~9-fold higher cellulase activity (measured as filter paper enzyme, FPase), ~8-fold higher xylanase (a major type of hemicellulase) activity, and ~4-fold higher total secreted proteins than wild-type strain 114-2 in cellulose-wheat bran (CW) medium, a typical cellulase producing medium for *P. decumbens*¹⁷ (Fig. 1B). Thus, the strain improvement has resulted in a mutant that produces more secreted proteins, especially cellulases and hemicellulases. In addition, strain 114-2 produces dark green conidia, while JU-A10-T produces much fewer and whitish-pink conidia on solid agar plates (Fig. 1C).

Global comparison of genomes of 114-2 and JU-A10-T. The genome of strain JU-A10-T was sequenced and assembled independently of that of 114-2 (Supplementary Table S1). The genome was assembled into 482 contigs totaling 30.69 Mb with 96.3% mapped onto the 8 chromosomes and the mitochondrial genome of 114-2 (Supplementary Fig. S1). The aligned DNA had an average of 1.4 single variations per kilobase (SNVs/kb; Supplementary Fig. S2A), less dense than that (7.8 SNVs/kb) between two *Aspergillus niger* strains¹⁸. Gene curation using transcriptomic data yielded 10,473 gene models in JU-A10-T (Supplementary Table S2). Strains 114-2 and JU-A10-T shared 9,599 proteins with an average amino acid identity of 99.55%, including 6,699 proteins with 100% identity over the full length (Supplementary Fig. S2B). The average protein identity was slightly lower than that (99.96%) between two *P. digitatum* isolates¹⁹. Proteins with sequence differences between 114-2 and JU-A10-T were enriched for those with transcription factor activities (P -value = 2.77×10^{-5}). Manual check of sequence alignments suggested that 140 of the 476 predicted transcription factors contained amino acid sequence differences between the strains (Supplementary Table S3). Strain-specific genes were mainly found in a few genomic regions, encoding primarily proteins of unknown function, transposases, vegetative incompatibility proteins, and proteins involved in biosynthesis of secondary metabolites (Supplementary Table S4). The features of strain-specific genes²⁰ indicate that the parent isolate 114 was likely a heterokaryon, and current strains 114-2 and JU-A10-T have been purified by subsequent transferring or screening processes (Fig. 1A).

Comparison of genes encoding lignocellulolytic enzymes. We have previously annotated 18 cellulases and 51 hemicellulases in 114-2 (ref. 13). JU-A10-T carried 66 of these enzymes, and it did not contain three adjacent hemicellulase genes in 114-2 scaffold 8 (PDE_08036, PDE_08037 and PDE_08038). The shared proteins were mostly identical. Only 26 amino acid differences were identified in 16 cellulases or hemicellulases between the strains, all occurring at non-conserved positions (Supplementary Table S5) that are not expected to affect enzyme activities²¹.

JU-A10-T increased secretion of lignocellulolytic enzymes and decreased secretion of amylases and proteases. Activity assays showed that extracellular cellulase and hemicellulase activities were both elevated, while the β -glucosidase activity was slightly reduced in JU-A10-T relative to those in 114-2 (Fig. 1B). The difference indicated possible altered secretome composition between the strains. When the secretomes of 114-2 and JU-A10-T were analyzed using liquid chromatography-tandem mass spectrometry (LC-MS/MS), 90 proteins were identified (Supplementary Table S6). Proteins involved in the degradation of cellulose, hemicellulose, starch and

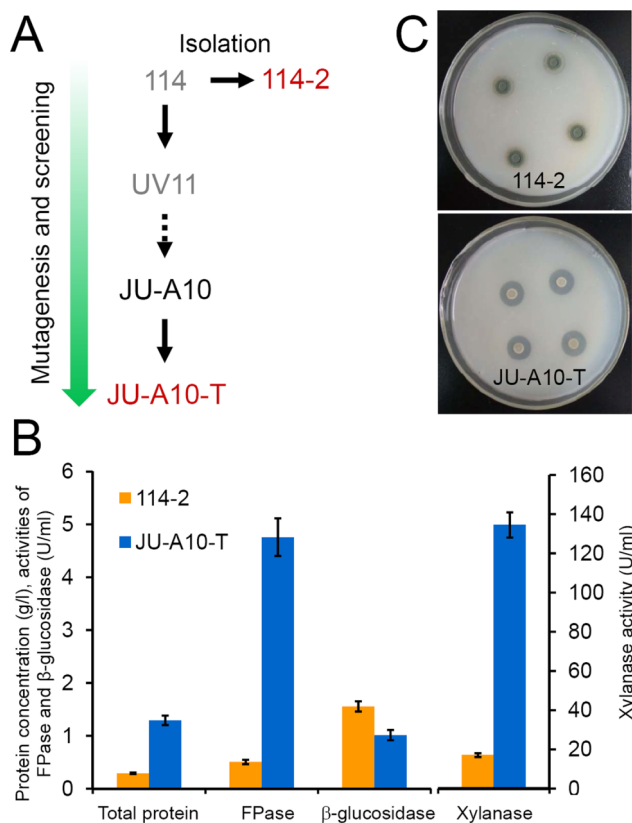


Figure 1 | *P. decumbens* mutagenesis and screening. (A) Genealogy of strains used. The two strains used for genome sequencing are labeled in red. Strains shown in gray have been lost over the years. (B) Production of lignocellulolytic enzymes by 114-2 and JU-A10-T. The two strains were grown in the cellulose-wheat bran medium for 4 days. FPase stands for filter paper enzyme activity. Error bars represent standard deviations of triplicate independent cultures. (C) Colony morphology of 114-2 and JU-A10-T on cellulose plates. Strain JU-A10-T generated larger cellulolytic halo than strain 114-2 did.



proteins were detected in the secretomes of both strains. However, the proportion of cellulases and hemicellulases increased, while the production of amylases, proteases and other proteins decreased markedly in the JU-A10-T secretome, according to peptide spectral counts of LC-MS/MS²² (Fig. 2A). The result was confirmed by comparing the two-dimensional electrophoresis map of JU-A10-T secretome (Supplementary Fig. S3A) with that of 114-2 (ref. 13). Nearly all the protein spots on gel for JU-A10-T were identified as lignocellulolytic enzymes. Consistently, extracellular amylase activity and protease activity of JU-A10-T were significantly lower than those of 114-2, respectively (Supplementary Fig. S3B). To further assess the changes in secretome composition, transcripts of the strains were analyzed (Supplementary Table S7). Transcripts of the 34 experimentally detected cellulases and hemicellulases accounted for 1.07% of total transcripts in strain 114-2, and the percentage increased to 9.03% in JU-A10-T (Fig. 2B and Tables S6). On the flip side, transcription levels of amylase and protease genes were lower in JU-A10-T. The expression of the principal β -glucosidase BGLI gene was essentially unchanged in JU-A10-T.

Genetic and transcriptional changes of transcription factors altered secretome composition in JU-A10-T. Like the first obtained mutant UV11, JU-A10-T showed CCR-resistant expression of cellulases and hemicellulases (e.g. higher expression in glucose

medium, Supplementary Fig. S4A). The gene *creA* (PDE_03168) in *P. decumbens*, a homolog of *T. reesei cre1* (ref. 7), encoding the key carbon catabolite repressor, had a frameshift mutation at the C-terminus in JU-A10-T (Supplementary Fig. S4B). The effect of CreA on the expression of extracellular hydrolytic enzymes was investigated by deleting the *creA* gene in strain 114-2. As expected, deletion of *creA* resulted in CCR-resistant expression of cellulases (Supplementary Fig. S4C). In addition, the $\Delta creA$ strain showed ~1.7-fold higher FPase activity and ~3.4-fold higher amylase activity than 114-2 in cellulose medium (Fig. 3), confirming the negative effect of CreA on cellulase expression under both repressing and inducing conditions²³.

Promoter regions (1.5-kb upstream region) of 11 cellulase genes contained 106 nucleotide differences between the strains (Supplementary Table S8). When the nucleotide differences were analyzed for their effects on putative binding motifs of CreA, one SNV in the promoter of a cellobiohydrolase gene *cel7A-1* was found to affect a putative CreA-binding site (two adjacent 5'-SYGGRG-3' motifs^{24,25}; Supplementary Fig. S5). Further, *Cel7A-1* had the highest fold change among the cellulases up-regulated in JU-A10-T (Supplementary Table S6). To investigate the mutation on transcription efficiency, the EGFP (enhanced green fluorescent protein) gene was fused to *cel7A-1* promoters from 114-2 and JU-A10-T, respectively, and then transformed into 114-2. Real-time quantitative RT-PCR analysis and microscopy analysis showed that the *cel7A-1* promoter from JU-A10-T had a ~2.6-fold higher transcriptional efficiency than the promoter from 114-2 (Fig. 4).

In *Aspergillus* species, transcriptions of amylase genes are coordinately activated by the transcription factor AmyR²⁶. The AmyR homologs in *P. decumbens* strains 114-2 and JU-A10-T (PDE_03964 and PDT_04193, respectively) were 100% identical, with a

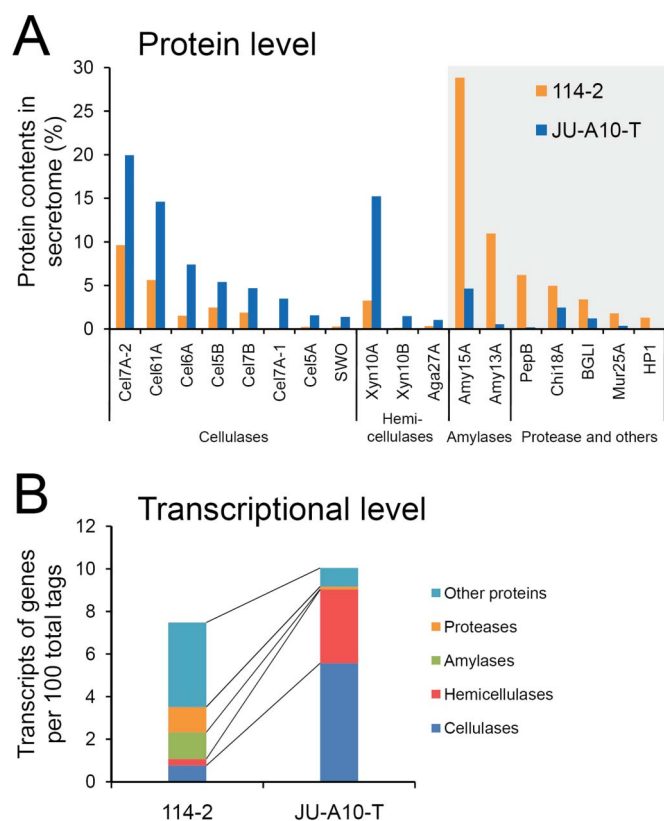


Figure 2 | Comparison of expression levels of secreted enzymes between strains 114-2 and JU-A10-T. (A) Secretome comparison. Protein abundance ratios are calculated according to peptide spectral counts in LC-MS/MS. Proteins with lower abundances in JU-A10-T are shown in gray background. The 18 major proteins were at least 1% in at least one of the two secretomes. Glycoside hydrolases (GHs) were named according to the CAZy families they were classified, except BGLI which belongs to GH family 3. Chi18A, a chitinase; Mur25A, a muramidase; HP1, a hypothetical protein. (B) Transcriptional level comparison. All the proteins detected in LC-MS/MS and 2DE-MS/MS were included. Detailed protein abundance ratios and transcription levels are listed in Supplementary Table S6.

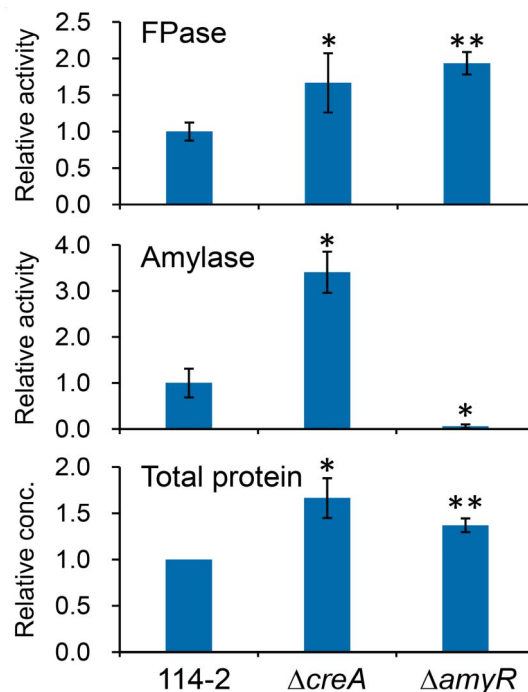


Figure 3 | Effect of deleting *creA* or *amyR* in strain 114-2 on the production of extracellular enzymes. Mycelia from 2% (w/v) glucose medium were grown in 1% (w/v) cellulose medium for another 48 h. Enzyme activities (U/ml) and protein concentrations were determined in the culture supernatant and expressed as relative values with those of 114-2 set at 1. Error bars represent standard deviations of triplicate independent cultures. Statistical significance of the difference between 114-2 and each gene deletion mutant is shown. *, $P < 0.05$; **, $P < 0.005$.

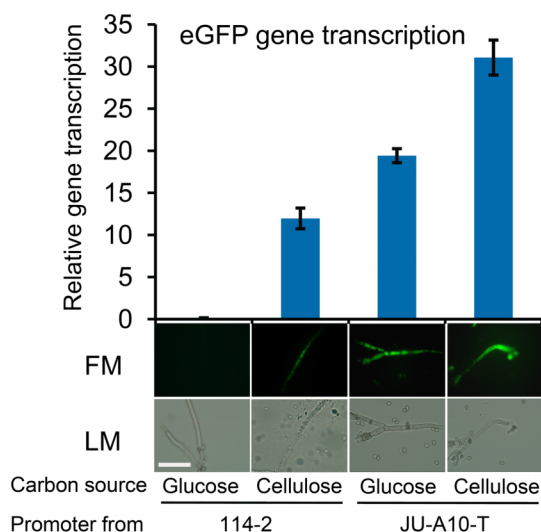


Figure 4 | Transcription efficiencies of *cel7A-1* promoters from strains 114-2 and JU-A10-T. Strains were grown in 1% (w/v) glucose medium or 1% (w/v) cellulose medium for 48 h. Transcription efficiency was analyzed by real-time quantitative RT-PCR of the reporter eGFP gene. Transcription levels of eGFP gene were normalized to 100-fold of those of β -actin. Error bars represent standard deviations of triplicate measurements. FM, fluorescence microscopy; LM, light microscopy. White bar = 10 μ m.

much lower gene transcription level in JU-A10-T than that in 114-2 (> 15-fold, Supplementary Dataset S1). Deletion of *amyR* in 114-2 dramatically decreased amylase activity by 94.2% (Fig. 3). Notably, the deletion also resulted in about 1.9-fold higher FPase activity, suggesting a negative role of AmyR in the expression of cellulase genes in strain 114-2.

Comparative transcriptome analysis revealed reorganized metabolism in JU-A10-T. The gene expression profiling data covered ~80% of the whole predicted genes (Supplementary Table S7), which allowed the study of genome-wide gene expression changes between the strains. Notably, JU-A10-T had remarkably more genes transcribed at low levels (< 10 transcripts per million clean tags) than 114-2 did (Fig. 5A). This indicated that some biological processes might be less active in JU-A10-T than those in 114-2. Correspondingly, 567 genes were significantly up-regulated, while up to 1,447 genes were significantly down-regulated in JU-A10-T (Supplementary Dataset S1).

Compared with 114-2, genes significantly up-regulated in JU-A10-T predominantly coded extracellular polysaccharide hydrolases (Fig. 5B and Supplementary Table S9). Genes involved in glycolysis and the citric acid cycle had minimal variations in expression, but the expression levels of genes for the pentose phosphate pathway (PPP) were up-regulated in JU-A10-T, such as the putative glucose-6-phosphate dehydrogenase (PDE_01924) gene which was up-regulated ~9 folds (Supplementary Table S10). The data suggest increased flux through PPP, which provides NADPH and precursors for amino acids biosynthesis. Interestingly, the genes responsible for channeling xylose and arabinose, the hydrolytic products of hemicellulose, into PPP for consumption were also over-expressed in JU-A10-T (Supplementary Table S10). For amino acid biosynthesis, the genes of the lysine and cysteine biosynthesis were up-regulated by 2 to 7 folds (Supplementary Table S11), which may facilitate the synthesis of the four major (hemi-)cellulolytic enzymes rich in lysine and/or cysteine (Supplementary Fig. S6). Ribosomal protein genes were significantly enriched in the up-regulated gene set (FDR = 7.31×10^{-5} , Supplementary Table S9). In addition, five genes involved in protein

folding were significantly up-regulated in JU-A10-T (Supplementary Table S12). Putative protein disulfide-isomerase PDE_06215 and molecular chaperone PDE_08980 genes were up-regulated by 6.0 and 2.7 folds, respectively, which may aid the hyper-production of secreted proteins in JU-A10-T.

The down-regulated gene set in JU-A10-T was significantly enriched for oxidoreductases involved in metabolism (Fig. 5B and Supplementary Table S9). Of the 173 down-regulated oxidoreductases, 141 were mapped to KEGG pathways²⁷, including 35 enzymes involved in degradation of amino acids (especially aromatic amino acids; Supplementary Table S13) and 29 genes responsible for biosynthesis of secondary metabolites. Further examination found that 104 out of 314 genes in predicted secondary metabolism gene clusters were significantly down-regulated, while only 11 were significantly up-regulated in JU-A10-T (Supplementary Table S14).

Discussion

Sequence analysis shows that the increased lignocellulolytic enzyme activities in mutant JU-A10-T are not due to the mutations in catalytic amino acid residues. This is not a surprise as the same conclusion has been reached with *T. reesei* mutant strains that over-produce cellulolytic enzymes^{10,11}. Our sequence analysis also points to the enriched mutations in transcription regulators. Through functional experiments in wild-type 114-2 as the reference strain, some of the transcription factors are shown to be involved in the hyper-producing characteristics of JU-A10-T. First, global transcription factor CreA has a frame-shift mutation at the C-terminus, changing the sequence of the last 16 amino acid residues. The *cre1* in *T. reesei* hyper-producing mutant Rut-C30 has a nonsense mutation that also enhances cellulase production⁷. This coincidence suggests that *creA* is a key target in genetic engineering of fungal strains for higher production of cellulolytic enzymes. Considering that glucose-resistant expression of cellulases has been observed in strain UV11 (Fig. 1A), the frameshift mutation in *creA* might occur in the early phase of mutagenesis and screening¹⁴.

Secondly, down-regulation of AmyR expression contributes to the hyper-production of cellulolytic enzymes in JU-A10-T. AmyR was previously regarded as an amylase-specific regulator and was recently shown to also regulate the expression of β -glucosidases and galactosidases in *A. niger*²⁸. In *A. oryzae*, mutation in *amyR* causes down-regulation of amylases and up-regulation of cellulolytic enzymes only in the presence of starch, and a CCR-involved mechanism is proposed to account for the increased cellulolytic enzymes²⁹. A CCR-involved mechanism is logic as AmyR activates the synthesis of amylases that convert starch to glucose, and the latter inhibits the production of cellulolytic enzymes through CCR. However, AmyR may also directly repress the transcription of cellulolytic enzyme genes, as shown in our medium without starch (Fig. 3). To the best of our knowledge, this is the first report of a regulatory effect of AmyR on cellulose-induced cellulase expression in fungi.

Comparative analysis of *N. crassa*²⁵ and *T. reesei*³⁰ strains with different production levels of cellulolytic enzymes have shown the up-regulation of protein synthesis and processing-related proteins in fungal strains that over-produce cellulolytic enzymes. Our global gene expression analysis show similar changes between JU-A10-T and 114-2. In addition, we have identified elevated transcription of genes involved in lysine and cysteine biosynthesis required for the production of major lignocellulolytic enzymes in JU-A10-T. In summary, mutations in the key gene expression regulators and promoter regions, together with other functional mutations to be identified, made strain JU-A10-T a hyper-yield and “specific” producer of lignocellulolytic enzymes compared with the versatile wild-type strain 114-2. Activities facilitating the production of lignocellulolytic enzymes are enhanced and other activities, such as the synthesis of secondary metabolites, are decreased. The results clearly demonstrate that we may target gene regulators and promoters with

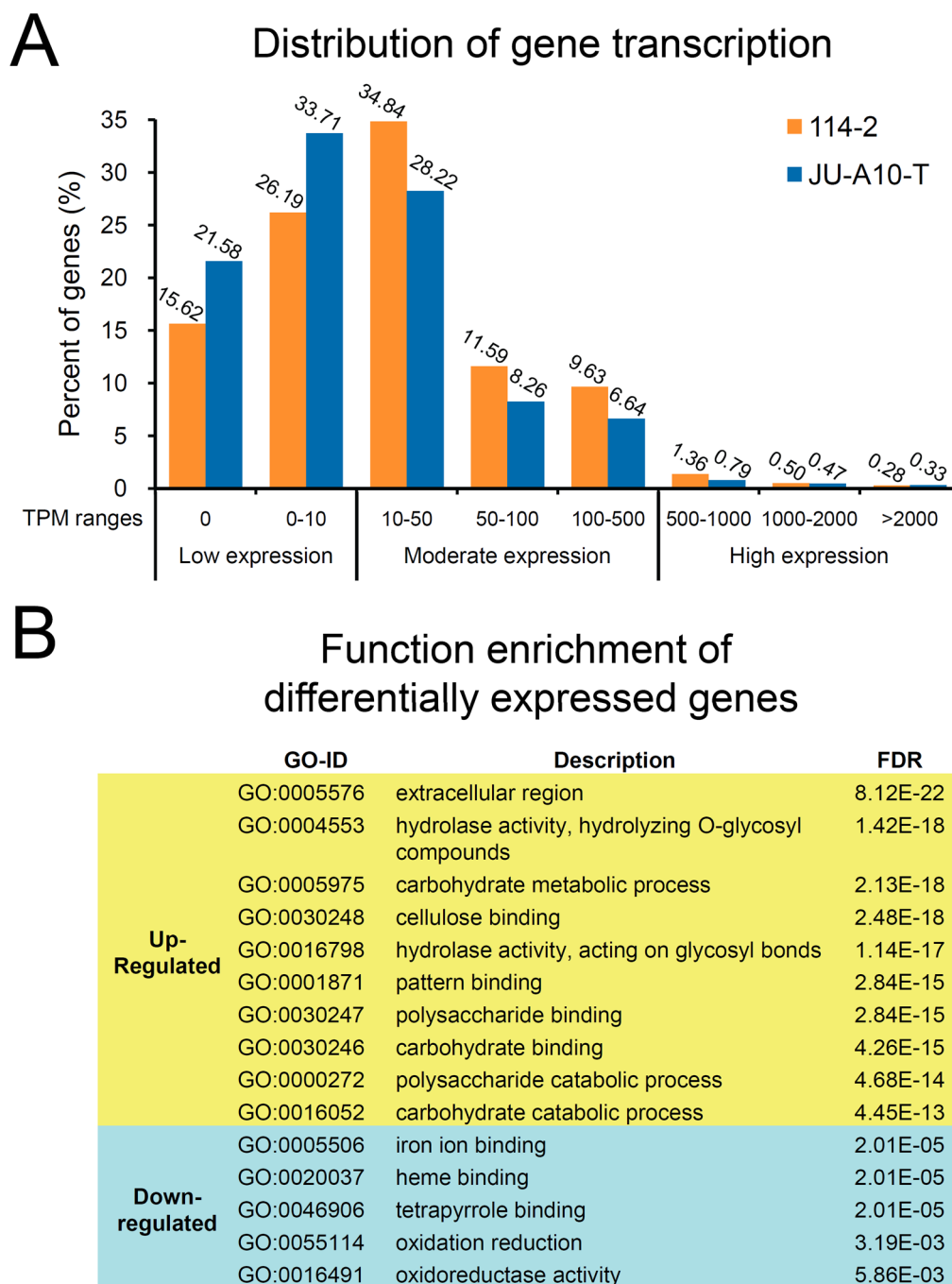


Figure 5 | Genome-wide gene expression changes between strains 114-2 and JU-A10-T. (A) Distribution of gene transcription levels. TPM, transcripts per million clean tags. Note that the percent of genes with very high transcription levels (TPM > 2,000) in JU-A10-T is higher than that in 114-2. (B) Gene Ontology (GO) enrichment of genes of significantly differential expression between JU-A10-T and 114-2. For up-regulated genes, only the top 10 significantly enriched GO terms are shown. The full results of gene function enrichment including gene IDs are listed in Supplementary Table S9.

minimal alterations of the genetic content but maximal effects in genetic engineering.

Methods

Strains and culture conditions. *P. decumbens* strains 114-2 (CGMCC 5302) and JU-A10-T were used in this study. All culture media were based on modified Mandels' salt solution (MMS), containing (g L⁻¹): KH₂PO₄ 3.0, NaNO₃ 2.6, MgSO₄·7H₂O 0.5, CaCl₂ 0.5, FeSO₄·7H₂O 0.0075, MnSO₄·H₂O 0.0025, ZnSO₄·7H₂O 0.0036 and CoCl₂·6H₂O 0.0037. Conidial suspensions were inoculated at a final concentration of 10⁶ per ml, and strains were grown at 30°C, 200 rpm (for liquid culture). For secretome analysis, digital gene expression profiling, and comparison of extracellular enzyme activities between 114-2 and JU-A10-T, strains were grown in MMS supplemented with 0.1% (w/v) peptone and 1% (w/v) microcrystalline cellulose plus

1% (w/v) wheat bran (CW medium) for indicated time periods. MMS supplemented with 0.1% (w/v) peptone and 2% (w/v) glucose (G medium) was also used in comparison of extracellular enzyme activities. For comparison of extracellular enzyme activities between 114-2 and transcription factor gene deletion mutants, conidia were pre-cultured in G medium for 24 h. Then, mycelia were collected by vacuum filtration, washed with sterile water and re-suspended in MMS supplemented with 1% (w/v) microcrystalline cellulose for further growth.

Protein concentration and enzyme assays. Protein concentration and extracellular hydrolase activities were assayed as previously described¹⁷. For FPase assay, dilutions of supernatant (0.5 ml) were incubated with Whatman No.1 filter paper (1 × 6 cm, 50 mg) in 1.0 ml of 0.2 M acetate buffer (pH 4.8) at 50°C for 60 min. Statistical significance tests were carried out using Microsoft Excel program with a one-tailed equal variance *t*-test.



Genome sequencing, assembly and annotation. The genome of JU-A10-T was sequenced with 454 GS FLX Titanium platform and the Illumina Genome Analyzer. Genome assembly was performed with the standard 454 assembler Newbler³¹ version 2.3 to generate contigs. Illumina mate-paired reads of strain JU-A10-T were mapped to contigs from 454 assembler to generate scaffolds. Gene models were predicted independently with a set of gene finders as performed in strain 114-2 (ref. 13), and then manually curated with 454-sequenced transcriptome sequences (NCBI Sequence Read Archive database accession no. SRA048522) and nr BLAST³² hits to justify intron-exon boundaries and UTR regions. Blast2GO³³ was used for Gene Ontology (GO)³⁴ and InterPro³⁵ annotation. Transcription factors were annotated according to the InterPro IDs in Fungal Transcription Factor Database³⁶. Secondary metabolism gene clusters were predicted with SMURF³⁷. Protein sequences from the eukaryotic genomes in KEGG GENES database²⁷ (Version 57) were compiled as BLAST library, and KO (KEGG Ortholog) identifiers were assigned with KOBAS³⁸ algorithm with a combination of thresholds (e -value $\leq 1e-5$ and rank < 5).

Genetic variation analysis. The genomes of 114-2 and JU-A10-T were aligned using mauve^{39,40} and Mummer⁴¹. In addition, sequencing reads of one strain were mapped to the genome of the other strain using BWA^{42,43}, Bowtie⁴⁴, SHRiMP⁴⁵, gsMapper³¹ and MOSAIK-ALIGNER (Version 1.1.0021, <http://code.google.com/p/mosaik-aligner/>). SNVs were called by Samtools and VarScan⁴⁶ via the resulted SAM or BAM files from the aligners. The SNVs were then filtered by composition complexity, where those with more than five homo-polymers in 21 bp-windows were discarded. SNVs supported by both reads level and genome level were retrieved as the final SNV set. Strain-specific genes were manually checked to remove false positive results caused by sequencing gaps or mistaken gene predictions.

Secretome analysis. Culture broths of strains grown in CW medium for 48 h were centrifuged at $12,000 \times g$ at 4°C for 20 min and the supernatants were analyzed by reversed-phase (RP) LC-MS/MS and two-dimensional electrophoresis (2DE)-MS/MS techniques. RP-LC-MS/MS and data analysis were performed as previously described²². The spectral counting method was used to determine the abundance of proteins in the secretomes⁴⁷. The secretome of JU-A10-T was also analyzed by 2DE using Ettan DIGE System (GE Healthcare) in dark as done in 114-2 (ref. 13). Spots of interest were manually excised, washed and trypsin-digested for MALDI-TOF/TOF mass spectrometry on 4700 Proteomics Analyzer (Applied Biosystems) in the positive ion reflector mode. An in-house *P. decumbens* protein sequence database was used for protein identification.

Digital gene expression profiling. Strains grown in CW medium for 41 h were used for total RNA extraction using the RNAsisoTM reagent (TaKaRa, Japan) according to the manufacturer's protocol. Digital gene expression profiling experiment based on Solexa sequencing⁴⁸ was performed by Beijing Genomics Institute (BGI) at Shenzhen, China. All clean tags obtained after raw data processing were mapped to the reference tag database (predicted transcripts plus downstream 300-nucleotide sequences) of the corresponding strain. Only sense expression was considered and no mismatch was allowed. The copy number of unambiguous tags (tags mapped to one single gene) for each gene was normalized to TPM (number of transcripts per million clean tags). Genes of significantly differential expressions were identified by a significance test⁴⁹ with combined thresholds ($FDR^{50} \leq 0.001$ and fold change ≥ 2). Blast2GO³³ was used for function enrichment analysis of gene sets with the threshold of $FDR \leq 0.05$.

Gene targeting of *creA* and *amyR*. The gene *creA* was deleted using $\Delta creA::hph$ targeting cassette carrying hygromycin B phosphotransferase (*hph*) expression cassette flanked by 5' and 3' sequence of *creA* gene⁵¹. Retransformation of $\Delta creA$ strain was performed using *creA::ptrA* targeting cassette carrying pyrithiamine resistance gene (*ptrA*)⁵² expression cassette flanked by *creA* expression cassette and downstream sequence of *creA* gene. The gene *amyR* was deleted in 114-2 using $\Delta amyR::ptrA$ targeting cassette carrying *ptrA* expression cassette flanked by 5' and 3' sequence of *amyR* gene. Construction of targeting cassettes and transformation of *P. decumbens* were performed as previously described⁵¹, and successful targeting was confirmed by Southern blot.

Promoter efficiency analysis. The reporter gene eGFP was introduced into the vector pDht/SK under control of *cel7A-1* promoters from 114-2 and JU-A10-T, respectively. The expression vectors were transformed into the recipient 114-2 via Agrobacterium-mediated fungal transformation. Transcription levels of eGFP and β -actin genes were analyzed by real-time quantitative PCR (Eppendorf, Germany), in which the primer pair 5'-AGTGGTTCAGCCGCTACCC-3' and 5'-GATGCCG-TTCTTCTGCTTGTG-3' were used for amplification of eGFP gene, and 5'-TGAG-GTCCCATCAACCC-3' and 5'-CACCAAGAGTCCAGCAGATA-3' were used for amplification of β -actin gene (PDE_01092).

Accession numbers. The Whole Genome Shotgun project of strain JU-A10-T has been deposited in DDBJ/EMBL/GenBank under the accession number AGI000000000. The digital gene expression profiling data have been deposited in NCBI's Gene Expression Omnibus under the GEO Series accession number GSE34288.

- Somerville, C. The billion-ton biofuels vision. *Science* **312**, 1277 (2006).
- Fernando, S., Adhikari, S., Chandrapal, C. & Murali, N. Biorefineries: current status, challenges, and future direction. *Energy & Fuels* **20**, 1727–1737 (2006).

- Sanchez, C. Lignocellulosic residues: biodegradation and bioconversion by fungi. *Biotechnol Adv* **27**, 185–194 (2009).
- Cherry, J. R. & Fidantsef, A. L. Directed evolution of industrial enzymes: an update. *Curr Opin Biotechnol* **14**, 438–443 (2003).
- Gusakov, A. V. Alternatives to *Trichoderma reesei* in biofuel production. *Trends Biotechnol* **29**, 419–425 (2011).
- Esterbauer, H., Steiner, W., Labudova, I., Hermann, A. & Hayn, M. Production of *Trichoderma cellulase* in laboratory and pilot scale. *Bioresour Technol* **36**, 51–65 (1991).
- Ilmen, M., Thrane, C. & Penttila, M. The glucose repressor gene *cre1* of *Trichoderma reesei*: Isolation and expression of a full-length and a truncated mutant form. *Mol Gen Genet* **251**, 451–460 (1996).
- Nitta, M. et al. A new Zn(II)(2)Cys(6)-type transcription factor BglR regulates beta-glucosidase expression in *Trichoderma reesei*. *Fungal Genet Biol* **49**, 388–397 (2012).
- Geysens, S. et al. Cloning and characterization of the glucosidase II alpha subunit gene of *Trichoderma reesei*: a frameshift mutation results in the aberrant glycosylation profile of the hypercellulolytic strain Rut-C30. *Appl Environ Microbiol* **71**, 2910–2924 (2005).
- Le Crom, S. et al. Tracking the roots of cellulase hyperproduction by the fungus *Trichoderma reesei* using massively parallel DNA sequencing. *Proc Natl Acad Sci U S A* **106**, 16151–16156 (2009).
- Vitikainen, M. et al. Array comparative genomic hybridization analysis of *Trichoderma reesei* strains with enhanced cellulase production properties. *BMC Genomics* **11**, 441 (2010).
- Gusakov, A. V. & Sinityn, A. P. Cellulases from *Penicillium* species for producing fuels from biomass. *Biofuels* **3**, 463–477 (2012).
- Liu, G. et al. Genomic and secretomic analyses reveal unique features of the lignocellulolytic enzyme system of *Penicillium decumbens*. *PLoS One* **8**, e55185 (2013).
- Qu, Y., Gao, P. & Wang, Z. Screening of catabolite repression-resistant mutants of cellulase producing *Penicillium* spp. *Acta Mycol Sinica* **3**, 238–243 (1984).
- Qu, Y., Zhao, X., Gao, P. & Wang, Z. Cellulase production from spent sulfite liquor and paper-mill waste fiber. *Appl Biochem Biotechnol* **28-29**, 363–368 (1991).
- Fang, X., Shen, Y., Zhao, J., Bao, X. & Qu, Y. Status and prospect of lignocellulosic bioethanol production in China. *Bioresour Technol* **101**, 4814–4819 (2010).
- Sun, X., Liu, Z., Qu, Y. & Li, X. The effects of wheat bran composition on the production of biomass-hydrolyzing enzymes by *Penicillium decumbens*. *Appl Biochem Biotechnol* **146**, 119–128 (2008).
- Andersen, M. R. et al. Comparative genomics of citric-acid-producing *Aspergillus niger* ATCC 1015 versus enzyme-producing CBS 513.88. *Genome Res* **21**, 885–897 (2011).
- Marcet-Houben, M. et al. Genome sequence of the necrotrophic fungus *Penicillium digitatum*, the main postharvest pathogen of citrus. *BMC Genomics* **13**, 646 (2012).
- Fedorova, N. D. et al. Genomic islands in the pathogenic filamentous fungus *Aspergillus fumigatus*. *PLoS Genetics* **4**, e1000046 (2008).
- Kumar, P., Henikoff, S. & Ng, P. C. Predicting the effects of coding non-synonymous variants on protein function using the SIFT algorithm. *Nat Protoc* **4**, 1073–1081 (2009).
- Li, R. X. et al. Localized-statistical quantification of human serum proteome associated with type 2 diabetes. *PLoS One* **3**, e3224 (2008).
- Aro, N., Pakula, T. & Penttila, M. Transcriptional regulation of plant cell wall degradation by filamentous fungi. *FEMS Microbiol Rev* **29**, 719–739 (2005).
- Cubero, B. & Scazzocchio, C. Two different, adjacent and divergent zinc finger binding sites are necessary for CREA-mediated carbon catabolite repression in the proline gene cluster of *Aspergillus nidulans*. *EMBO J* **13**, 407–415 (1994).
- Sun, J. & Glass, N. L. Identification of the CRE-1 cellulolytic regulon in *Neurospora crassa*. *PLoS One* **6**, e25654 (2011).
- Petersen, K. L., Lehmbeck, J. & Christensen, T. A new transcriptional activator for amylase genes in *Aspergillus*. *Mol Gen Genet* **262**, 668–676 (1999).
- Kanehisa, M., Goto, S., Furumichi, M., Tanabe, M. & Hirakawa, M. KEGG for representation and analysis of molecular networks involving diseases and drugs. *Nucleic Acids Res* **38**, D355–360 (2010).
- vanKuyk, P. A., Benen, J. A., Wosten, H. A., Visser, J. & de Vries, R. P. A broader role for AmyR in *Aspergillus niger*: regulation of the utilisation of D-glucose or D-galactose containing oligo- and polysaccharides. *Appl Microbiol Biotechnol* **93**, 285–293 (2012).
- Watanabe, J. et al. Loss of *Aspergillus oryzae amyR* function indirectly affects hemicellulolytic and cellulolytic enzyme production. *J Biosci Bioeng* **111**, 408–413 (2011).
- Foreman, P. K. et al. Transcriptional regulation of biomass-degrading enzymes in the filamentous fungus *Trichoderma reesei*. *J Biol Chem* **278**, 31988–31997 (2003).
- Margulies, M. et al. Genome sequencing in microfabricated high-density picolitre reactors. *Nature* **437**, 376–380 (2005).
- Altschul, S. F., Gish, W., Miller, W., Myers, E. W. & Lipman, D. J. Basic local alignment search tool. *J Mol Biol* **215**, 403–410 (1990).
- Conesa, A. et al. Blast2GO: a universal tool for annotation, visualization and analysis in functional genomics research. *Bioinformatics* **21**, 3674–3676 (2005).
- Ashburner, M. et al. Gene ontology: tool for the unification of biology. *Nat Genet* **25**, 25–29 (2000).



35. Hunter, S. *et al.* InterPro in 2011: new developments in the family and domain prediction database. *Nucleic Acids Res* **40**, D306–312 (2012).
36. Park, J. *et al.* FTED: an informatics pipeline supporting phylogenomic analysis of fungal transcription factors. *Bioinformatics* **24**, 1024–1025 (2008).
37. Khaldi, N. *et al.* SMURF: Genomic mapping of fungal secondary metabolite clusters. *Fungal Genet Biol* **47**, 736–741 (2010).
38. Mao, X., Cai, T., Olyarchuk, J. G. & Wei, L. Automated genome annotation and pathway identification using the KEGG Orthology (KO) as a controlled vocabulary. *Bioinformatics* **21**, 3787–3793 (2005).
39. Darling, A. C., Mau, B., Blattner, F. R. & Perna, N. T. Mauve: multiple alignment of conserved genomic sequence with rearrangements. *Genome Res* **14**, 1394–1403 (2004).
40. Darling, A. E., Mau, B. & Perna, N. T. progressiveMauve: multiple genome alignment with gene gain, loss and rearrangement. *PLoS One* **5**, e11147 (2010).
41. Kurtz, S. *et al.* Versatile and open software for comparing large genomes. *Genome Biol* **5**, R12 (2004).
42. Li, H. & Durbin, R. Fast and accurate short read alignment with Burrows-Wheeler transform. *Bioinformatics* **25**, 1754–1760 (2009).
43. Li, H. & Durbin, R. Fast and accurate long-read alignment with Burrows-Wheeler transform. *Bioinformatics* **26**, 589–595 (2010).
44. Langmead, B., Trapnell, C., Pop, M. & Salzberg, S. L. Ultrafast and memory-efficient alignment of short DNA sequences to the human genome. *Genome Biol* **10**, R25 (2009).
45. Rumble, S. M. *et al.* SHRiMP: accurate mapping of short color-space reads. *PLoS Comput Biol* **5**, e1000386 (2009).
46. Koboldt, D. C. *et al.* VarScan: variant detection in massively parallel sequencing of individual and pooled samples. *Bioinformatics* **25**, 2283–2285 (2009).
47. Chundawat, S. P. *et al.* Proteomics-based compositional analysis of complex cellulase-hemicellulase mixtures. *J Proteome Res* **10**, 4365–4372 (2011).
48. AC't Hoen, P. *et al.* Deep sequencing-based expression analysis shows major advances in robustness, resolution and inter-lab portability over five microarray platforms. *Nucleic Acids Res* **36**, e141–e141 (2008).
49. Audic, S. & Claverie, J. M. The significance of digital gene expression profiles. *Genome Res* **7**, 986–995 (1997).
50. Benjamini, Y. & Yekutieli, D. The control of the false discovery rate in multiple testing under dependency. *Ann Stat*, 1165–1188 (2001).
51. Li, Z., Du, C., Zhong, Y. & Wang, T. Development of a highly efficient gene targeting system allowing rapid genetic manipulations in *Penicillium decumbens*. *Appl Microbiol Biotechnol* **87**, 1065–1076 (2010).
52. Kubodera, T., Yamashita, N. & Nishimura, A. Transformation of *Aspergillus* sp. and *Trichoderma reesei* using the pyrithiamine resistance gene (*ptrA*) of *Aspergillus oryzae*. *Biosci Biotechnol Biochem* **66**, 404–406 (2002).

Acknowledgements

This study was supported by grants from National Basic Research Program of China (Grant no. 2011CB707403), National Natural Sciences Foundation of China (Grant no. 31030001) and International S&T Cooperation Program of China (2010DFA32560). We thank Bingqiang Liu and Yang Li for kind help in differential gene expression analysis.

Author contributions

Y. Qu, Z.Z., T.W. and G.-P.Z. supervised the study and designed main experiments. G.Z., M.C., K.Z. and G.L. isolated DNA and RNA for sequencing. J.L., H.Z. and S.W. performed genome sequencing. L.Z. performed genome assembling and gene annotation. L.Z., G.Z., G.L., Y. Qin and L.M. participated in accurate adjustment of gene models. X.Y., J.Z. and L.C. prepared secreted protein samples for LC-MS/MS. G.Z. and R.L. performed efficiency analysis of promoters. X.W. and G.L. performed enzyme assays and 2DE analysis. Z.L. performed targeted gene deletion. G.L., L.Z. and G.Z. analyzed data and drafted the manuscript. H.X., X.B., X.F., L.W., Y.Z. and W.L. commented on the manuscript. Z.Z., L.X., C.W., G.-P.Z. and Y. Qu revised the manuscript.

Additional information

Supplementary information accompanies this paper at <http://www.nature.com/scientificreports>

Competing financial interests: The authors declare no competing financial interests.

License: This work is licensed under a Creative Commons Attribution-NonCommercial-NoDerivs 3.0 Unported License. To view a copy of this license, visit <http://creativecommons.org/licenses/by-nc-nd/3.0/>

How to cite this article: Liu, G.D. *et al.* Long-term strain improvements accumulate mutations in regulatory elements responsible for hyper-production of cellulolytic enzymes. *Sci. Rep.* **3**, 1569; DOI:10.1038/srep01569 (2013).